

# **Erbium Doped AlGaAs/GaAs Quantum Wells**

**Galina Khitrova and Hyatt M. Gibbs**  
*Optical Sciences Center*  
1630 E. University Boulevard  
University of Arizona  
Tucson, AZ 85721-0094

**AFOSR**  
**Final Report for F49620-95-1-0381**  
**For the Period 6-1-95 through 3-31-97**

**19970606 146**

---

## **Abstract**

The possibility of enhancing the luminescence efficiency of Er ions embedded in a semiconductor was investigated by growing about forty erbium-doped InGaAs/GaAs and GaAs/AiGaAs multiple quantum well samples by molecular beam epitaxy. The idea was to enhance the semiconductor-to-erbium transfer when the quantum-well and erbium-ion transition energies are equal. Photoluminescence of Er ions and Er induced defects was studied at liquid helium and higher temperatures. A strong diffusion of erbium and interdiffusion of Ga and Al ions was observed, leading at high erbium concentrations to the degradation of the QW's and macroscopic average leveling of Er and Al concentrations over the whole grown structure. From high-resolution photoluminescence spectra the existence of three types of Er centers was deduced which differ by position of fine structure lines, photoluminescence lifetimes, and temperature dependence. These centers cause three types of carrier traps with binding energies of 20, 50, and 400 meV. Evidence is given that carriers captured into these traps control the Auger excitation of Er ions assisted by multiphonon emission. Er luminescence associated with the 400 meV trap is still detectable at room temperature. This grant was terminated abruptly after 71% of the funding was received, purportedly for financial rather than scientific reason.

## **Erbium Doped AlGaAs/GaAs Quantum Wells**

### ***Introduction***

In this report we present the results of detailed studies of Er-doped GaAs/AlGaAs structures grown by MBE. Using secondary ion mass spectroscopy (SIMS) data, absorption measurements, and photoluminescence (PL) measurements, we show that the introduction of erbium into GaAs/AlGaAs quantum well structures in the process of growth by MBE leads to efficient diffusion of Er and interdiffusion of Ga and Al. In the limit of high concentrations of erbium inserted during MBE growth, we have observed the degradation of the quantum structures and practically homogeneous distribution of erbium, gallium, and aluminum over the bulk of the sample (within the measurement limits of our instruments). We show that the doping of our quantum structures with erbium leads to a formation of three defect levels in the AlGaAs bandgap and that charge carriers localized at these levels determine the processes that excite the erbium ions. We have actually succeeded in exciting erbium ions via high excited states. This process favors the development of lasers using radiative transitions in the f-shell of erbium ions inserted into semiconductor structures.

### ***Experimental Procedure***

#### **Sample preparation**

The erbium-doped structures examined here were grown in the group's Riber 32P MBE machine by Professors Galina Khitrova and Hyatt Gibbs on 625- $\mu\text{m}$  GaAs substrates

---

with a substrate temperature of  $\sim 600^\circ\text{C}$ . The structures we label Er20 to Er23 consisted of an  $\text{Al}_{0.3}\text{Ga}_{0.7}\text{As}$  etch stop layer  $0.6\ \mu\text{m}$  thick, then 50 quantum wells each consisting of a  $10\ \text{nm}$   $\text{GaAs:Er}$  well and  $21\ \text{nm}$   $\text{AlGaAs}$  barriers with the Er cell temperature at  $450^\circ\text{C}$  (and shutter closed),  $900^\circ\text{C}$ ,  $870^\circ\text{C}$ , and  $930^\circ\text{C}$ , respectively (variation of the temperature of the erbium cell changes the erbium concentration). In all the samples there were also  $0.9\ \text{nm}$   $\text{AlAs}$  spikes at each end of the barriers separating the  $\text{GaAs:Er}$  and  $\text{AlGaAs}$ . On top of the 50 QW's there was another identical  $0.6\ \mu\text{m}$   $\text{AlGaAs}$  window to symmetrize the strain. Finally about  $7\ \text{nm}$  of  $\text{GaAs}$  was grown on top to prevent the  $\text{AlGaAs}$  from oxidizing. This QW structure is schematically shown in Fig. 1.

The structure Er26 consisted of  $8\ \text{nm}$   $\text{GaAs:Er}$  ( $900^\circ\text{C}$ ) layers separated by  $22\ \text{nm}$  of undoped  $\text{GaAs}$  repeated 50 times with  $300\ \text{nm}$  of  $\text{GaAs}$  on top. Er25 and Er34 are like Er20 except that they have no  $\text{AlAs}$  spikes. They also vary from Er20 in that Er25 had Er ( $900^\circ\text{C}$ ) in the  $\text{GaAs}$  well only and Er34 in the  $\text{AlGaAs}$  barrier only. Sample Er29 consisted of Er ( $900^\circ\text{C}$ ) homogeneously doped into  $1.7\ \mu\text{m}$  of  $\text{Al}_{0.3}\text{Ga}_{0.7}\text{As}$ . The Er concentrations measured by SIMS of these samples are presented in Table 1.

---

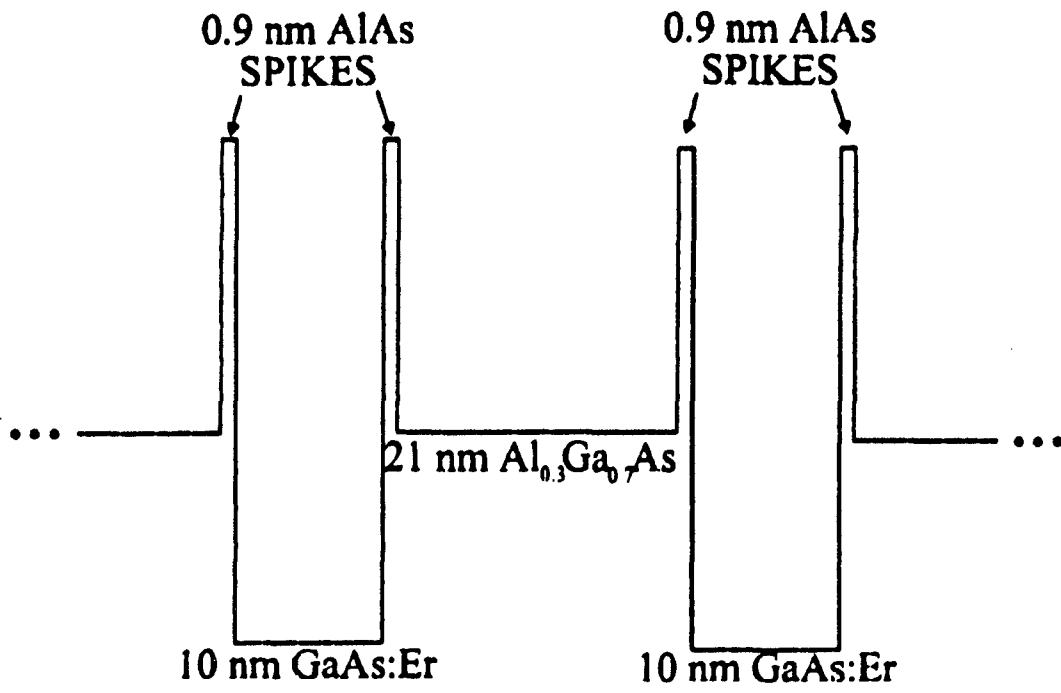


**Figure 1** Conduction band structure for Er20, 21, 22, and 23.

The dependence of the erbium concentration on the temperature of the source during growth (deduced from our measurements) can be summarized approximately by the formula:

$$N_{Er} = N \exp\left(-\frac{E_b}{kT}\right) \quad (3.1)$$

where  $N = 2.85 \times 10^{34} \text{ cm}^{-3}$  and  $E_b = 3.6 \text{ eV}$  which is similar to the activation energy  $E_b = 3.3 \text{ eV}$  of erbium evaporation from the metal source (see Fig. 2).

### Experimental measurements

SIMS measurements were made at the facilities in St. Petersburg and gave a depth resolution of 5 nm. Low temperature (1.8K) photoluminescence spectra of the structures

Sample number	Temperature of erbium source (°C)	Erbium concentration from SIMS ( $\text{cm}^{-3}$ )	Comments
Er20	No erbium		
Er21	900	$9 \times 10^{18}$	Er in QW
Er22	870	$3 \times 10^{18}$	Er in QW
Er23	930	$2.2 \times 10^{19}$	Er in QW
Er25	900	$7 \times 10^{18}$	Er in QW
Er26	900	$4 \times 10^{18}$	GaAs:Er
Er29	900	$9 \times 10^{18}$	AlGaAs:Er
Er34	900	$6 \times 10^{18}$	Er in barrier

**Table 1.** Erbium concentrations, determined by SIMS, of the grown structures

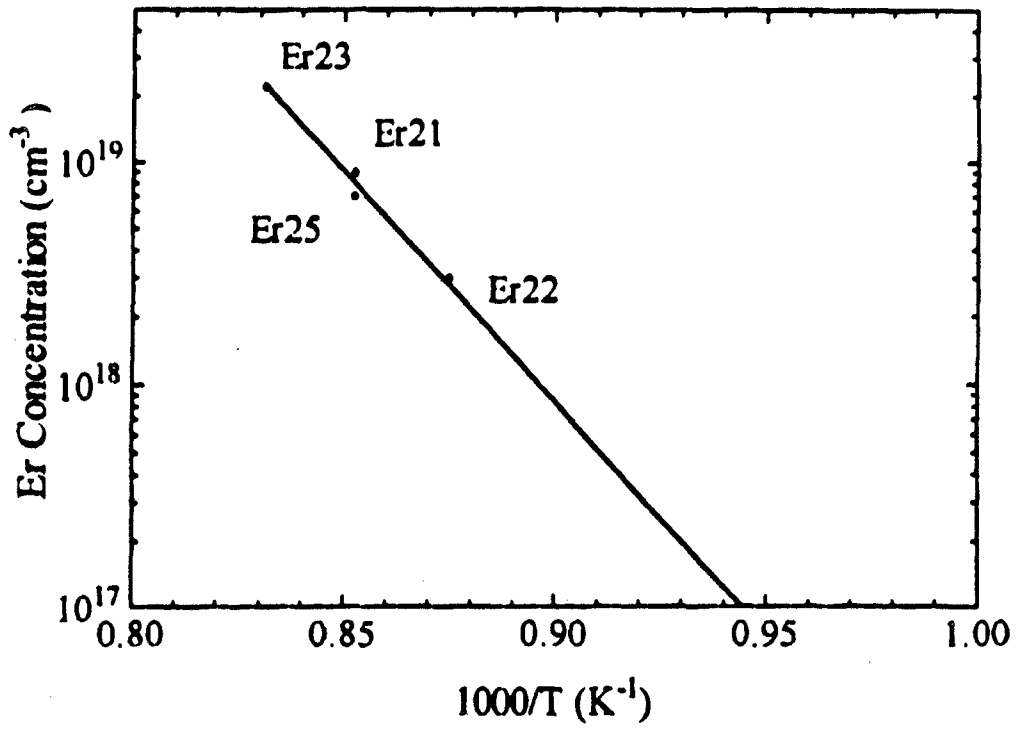


Figure 2 Erbium concentration as a function of Er cell temperature.

were measured immersed in liquid helium. The spectra were analyzed with an 822 mm double grating spectrometer and detected by a liquid-nitrogen-cooled germanium photodetector. Excitation was provided by an argon cw laser using the 488 nm line with pump powers up to 40 mW. PL lifetimes were determined by a phase shift method in which a phase sensitive detector was used to measure the phase difference between the PL and pump light signals.

Absorption spectra of the structures were performed with the GaAs substrate chemically etched away to prevent absorption of the transmitted light that was below the bandedge of GaAs. The techniques that we used to accomplish this etching are described by LePore (1981). The spectra were measured with the samples at 4K in a liquid-helium open-cycle cryostat and were resolved by a 1/8<sup>m</sup> meter scanning spectrometer and detected by a liquid nitrogen-cooled germanium photodiode. The setup is shown in Fig. 3.

Temperature dependencies of the intensities of different spectral lines were studied using two slightly different measurement setups, one in transmission and the other in reflection. Both setups used a closed-cycle helium cryostat with temperature control from 10K to above room temperature. Excitation was provided by an argon cw laser running on multiple lines with pump powers up to 100 mW. This laser beam was modulated by a chopper blade rotating at ~22 Hz. This slow speed was necessary because of the long lifetime of the erbium PL. The spectra were resolved in a scanning 3/4 m spectrometer with a liquid-nitrogen-cooled germanium photodiode at the output slit. The electrical output of the detector was sent to a preamplifier and then to a lock-in amplifier

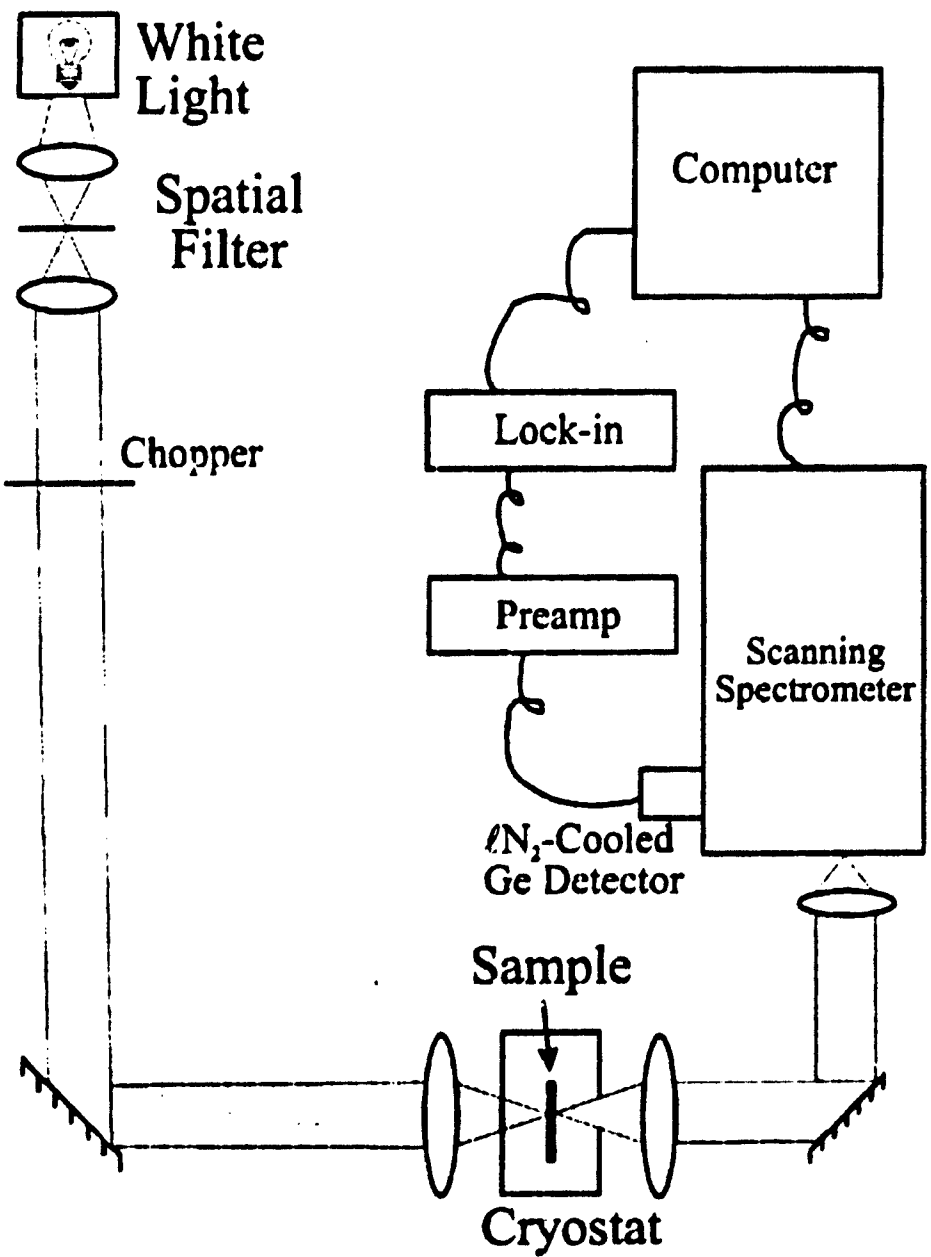


Figure 3 Absorption measurement setup.

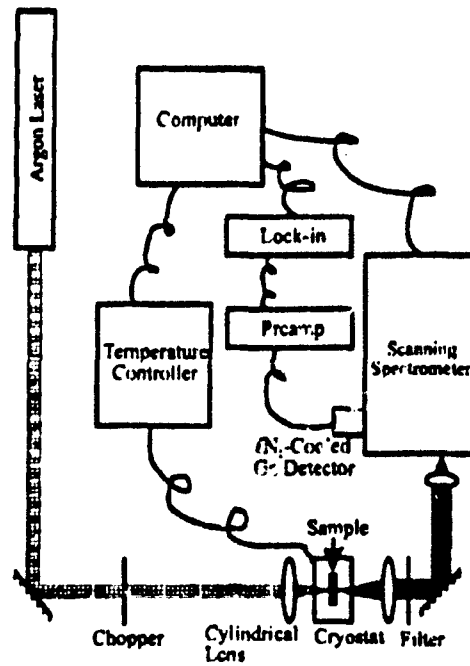
where the PL signal was extracted. Various colored filters were placed in the PL beam to prevent any laser light from entering the spectrometer, as well as to prevent any second order light from the spectrometer's grating giving false results.

The temperature controller, spectrometer, and lock-in amplifier were all interfaced to a computer program that allowed the taking of multiple spectra scans at different temperatures. To reduce the noise of the weaker signals, many scans at the same temperature were added together. Some of the temperature data series presented here took more than a non-interrupted 24-hour period to complete. The only restriction on the length of the measurement was determined by the need of refilling the liquid-nitrogen dewar of the photodiode every seven hours. This measurement time could be extended by pausing the measurement program, refilling the nitrogen, and then continuing.

Because the PL from the Er in our samples remained weak, many different strategies were tried to increase the measured signal. We finally used a cylindrical focusing lens for the argon pump laser to create a linear focus on the input slit of the spectrometer rather than a spot. Collecting the PL from the polished back side of the sample was then needed to gather as much light as possible to send into the spectrometer. This required the transmission type geometry that is pictured in Fig. 4a.

For all of the PL-versus-temperature measurements we left the substrate on to reduce heating. When we needed to look at PL that was below the bandedge of GaAs we used the reflection geometry shown in Fig. 4b. Reflection was required because, in the transmission geometry, all of the light of interest would have been absorbed by the GaAs substrate.

a) Transmission PL Setup



b) Reflected PL Setup

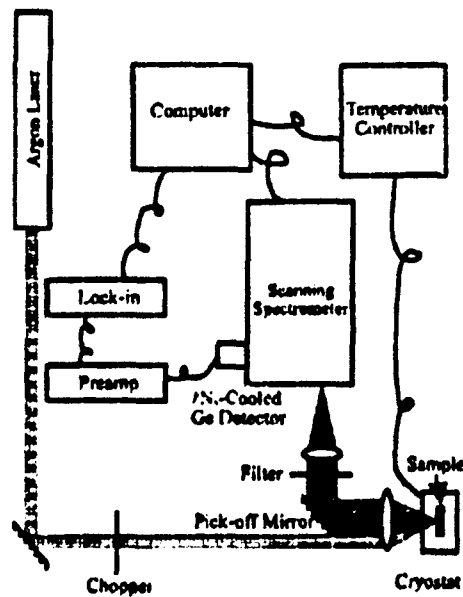


**Figure 4** Temperature dependent PL measurement setups for a) transmission geometry and b) reflection geometry.

## **Experimental Results**

### **Er-induced Ga-Al interdiffusion and Er diffusion**

The SIMS profile for the Er26 sample (GaAs:Er), shown in Fig. 5, shows a concentration of  $4 \times 10^{18} \text{ cm}^{-3}$  completely independent of position, contrary to opening and closing of the Er shutter during growth. It is clear that no erbium layers exist in the structure; complete leveling of the erbium concentration occurred indicating a high diffusion coefficient of erbium in bulk GaAs grown by MBE in contrast to the case of introduction of erbium by diffusion techniques.

In Fig. 6 the SIMS profiles are presented for three samples in the order of increasing erbium concentration which was introduced only into the GaAs QW layers. While for Er20 (no Er) distinct QW's are seen in the SIMS picture, for Er21 they are less pronounced, and in Er23 QW's are no longer seen with our SIMS resolution. In Er23 ( $N_{\text{Er}} = 2.2 \times 10^{19} \text{ cm}^{-3}$ ) no SIMS modulation is seen for either Ga, Al or Er. Thus, the interdiffusion of gallium and aluminum and diffusion of erbium depends directly on the concentration of erbium ions. Since SIMS has a limited spatial resolution there is also the possibility that Er causes the growth to become so wavy or rough that no modulation of the average density is seen even though QW's still exist to some extent. However, PL spectra independently indicate that the Er and Al end up together.

In Fig. 7a the PL spectrum of the Er26 sample is presented in the spectral region of erbium PL (1.5 - 1.6  $\mu\text{m}$ ). This sample is erbium-doped bulk GaAs, erbium being inserted into the semiconductor during MBE growth of the GaAs layer every 8 nm

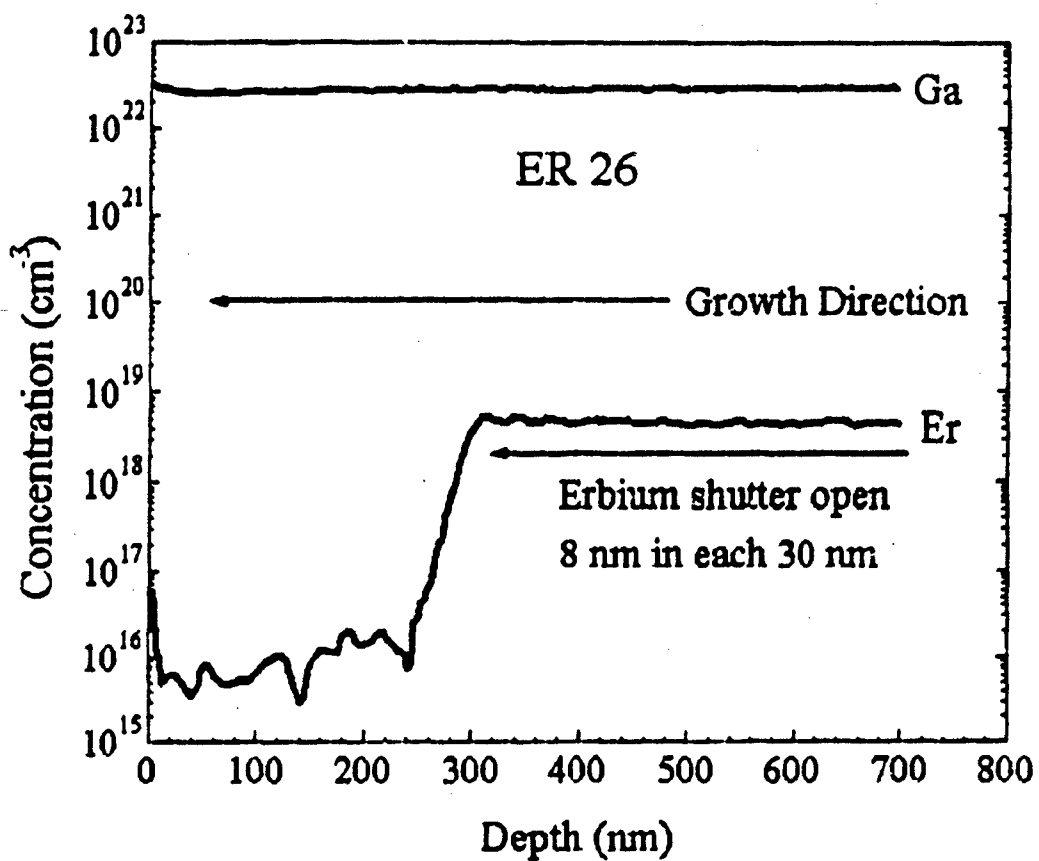


Figure 5 SIMS profile for Er<sub>26</sub>.

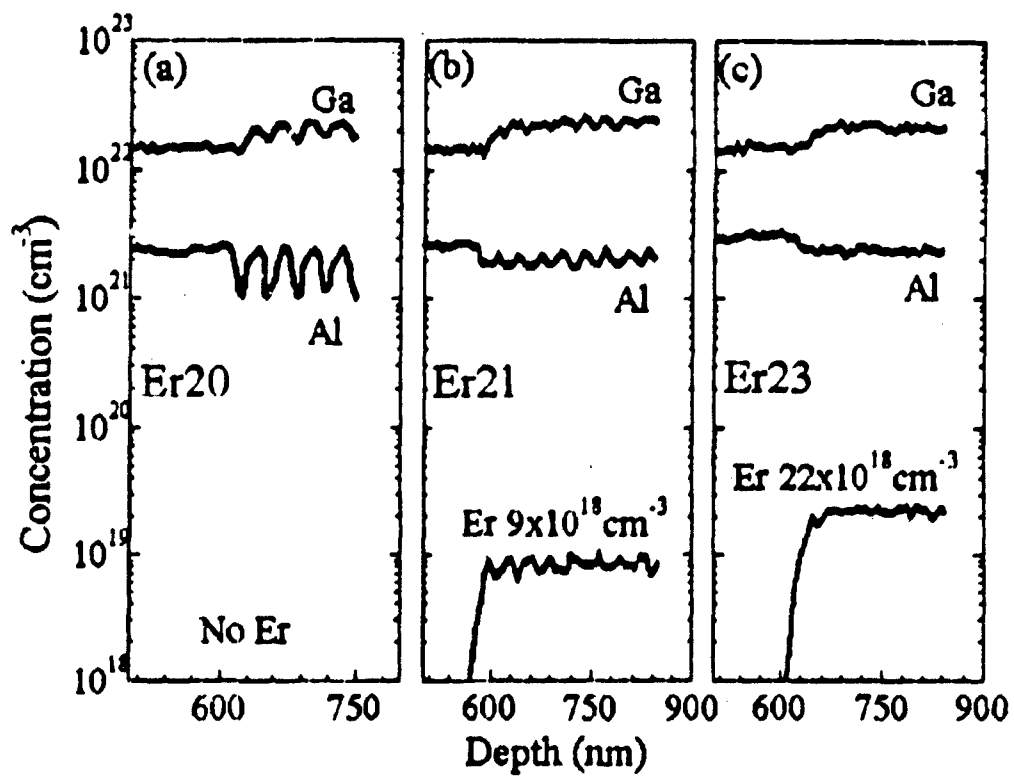


Figure 6 SIMS profiles for a) Er 20, b) Er21, and c) Er23.

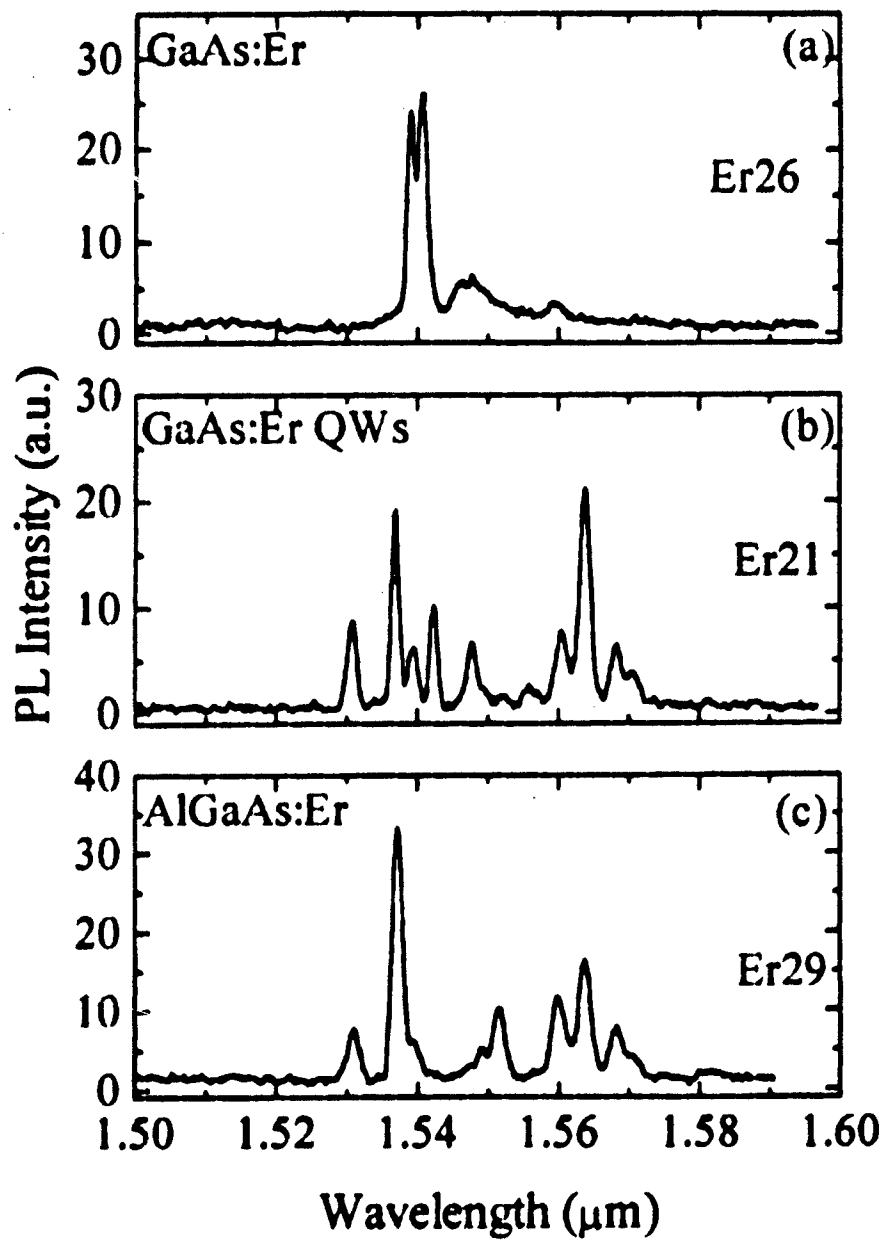


Figure 7 High resolution PL spectra of a) Er26, b) Er21, and c) Er29.

in each 30 nm. The positions of erbium PL lines corresponding to the  $^4I_{13/2} \rightarrow ^4I_{15/2}$  transition in the f-shell of the erbium ion are in good agreement with the literature data for GaAs without additional doping [Elsaesser *et al.* (1993)].

In Fig. 7b the PL spectrum of the Er21 sample is shown. In this case erbium was introduced into the QW's only (into GaAs). Obviously this spectrum differs significantly from the GaAs:Er PL spectrum, but strongly resembles the PL spectrum of the Er29 sample (Fig. 7c) where erbium was introduced into bulk AlGaAs (PL of MBE-grown Er-doped  $Al_xGa_{1-x}As$  was first observed by Zhang *et al.* (1993)). This point corroborates the previously drawn conclusion that upon the introduction of erbium into the GaAs QW's only, interdiffusion of gallium and aluminum takes place.

There seems to exist an interaction between erbium and aluminum ions that drives erbium into aluminum-rich regions and aluminum into the erbium-doped part of the structure. The evidence for erbium's preference to have an Al environment instead of a Ga environment can be seen by comparing the SIMS of Er21 (Al spikes around GaAs:Er well, showing weak Er SIMS modulation), Er25 (no AlAs spikes between AlGaAs barriers and GaAs:Er well, showing no Er SIMS modulation), and Er34 (no AlAs spikes between AlGaAs:Er barriers and GaAs well, showing stronger Er SIMS modulation) shown in Figs. 6b and 8. Qualitatively this shows that if the Er is placed in AlGaAs, it does not leave it to go into GaAs; if placed in GaAs, some of it ends up in AlGaAs also. These data show that Er binds more strongly to Al than Ga.

The absorption spectra of Fig. 9 give further support to the picture of an erbium-aluminum interaction. The spectrum of Er20 clearly shows the 2-dimensional staircase-

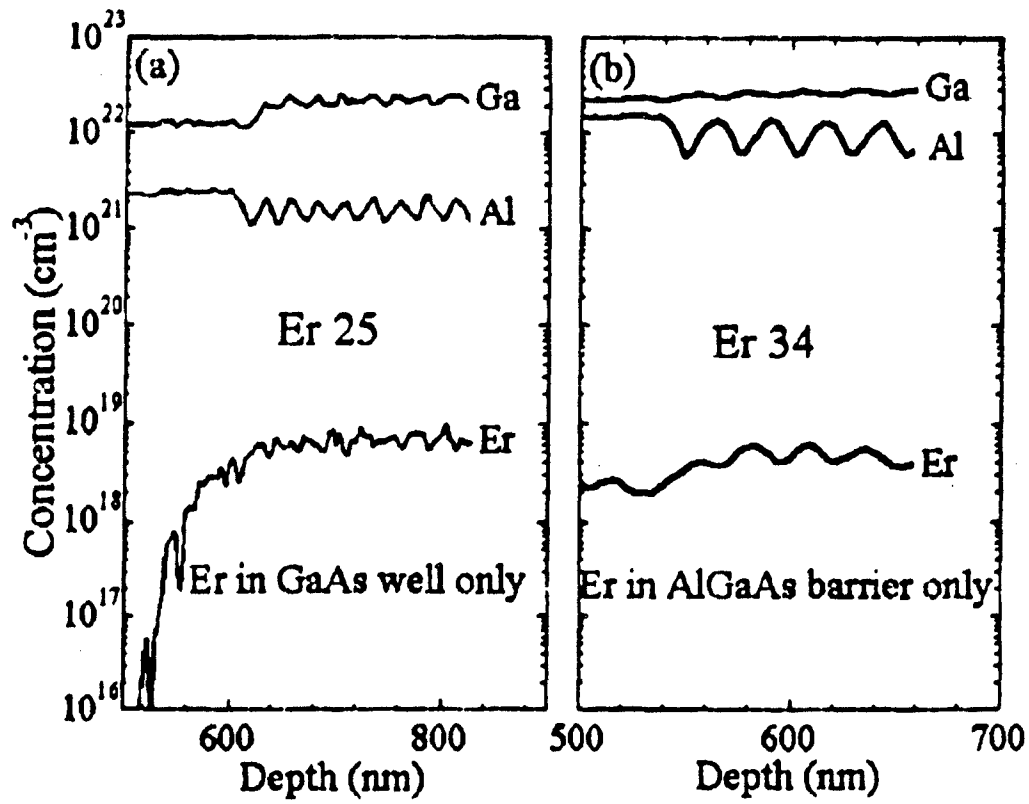
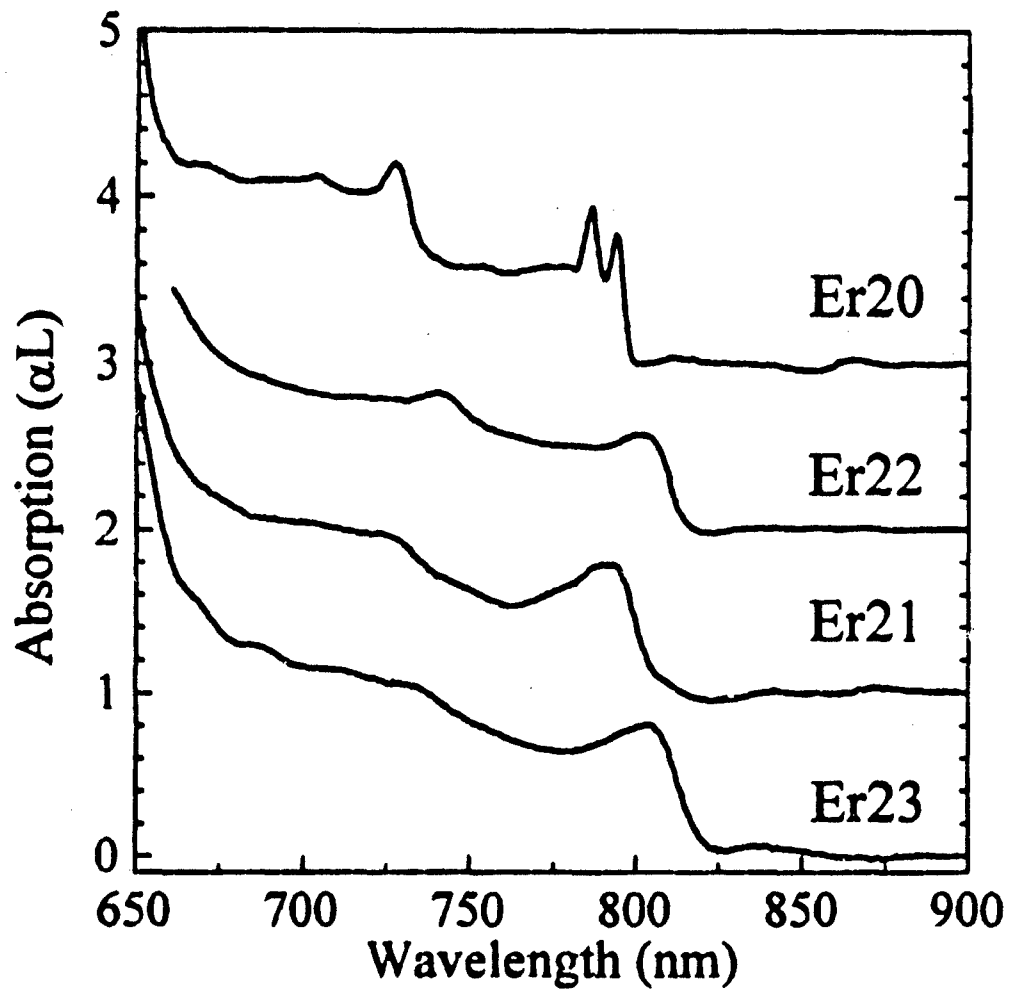


Figure 8 SIMS profiles for a) Er25 and b) Er34.



**Figure 9** Absorption spectra for Er20, Er22, Er21, and Er23. Curves are separated vertically by 1.0 for clarity.

like density of states for  $n = 1, 2$ . As the erbium concentration increases in Er22 and Er21, the staircase absorption becomes less apparent. In Er23, which has the highest erbium concentration, the absorption begins to follow the 3-dimensional density of states, close to that of bulk GaAs, but slightly higher in bandgap. This is consistent with Er-Al clusters in almost bulk GaAs, rather than  $\text{Al}_{0.25}\text{Ga}_{0.75}\text{As}$  which would result from a homogeneous interdiffusion of the Al. If Al diffusion into the GaAs wells did not form clusters, the band edge energy would go up dramatically with Al concentration but Fig. 9 shows it does not.

Further evidence for an Er-Al interaction comes from the PL spectra of Fig. 7. As observed earlier, even though Er was introduced only into the GaAs layers in structure Er21, the Er PL spectrum at  $1.54 \mu\text{m}$  (Fig. 7b) is characteristic of AlGaAs (Fig. 7c) which is much more complex than that of Er in GaAs (Fig. 7a). It should be noted that we have observed erbium PL spectra resembling the spectra of AlGaAs:Er even in the samples with very small erbium concentrations ( $< 10^{17} \text{ cm}^{-3}$ ) inserted into the GaAs QW's so that the quantum well structure was well preserved. These facts clearly indicate an Al-Er interaction.

The phenomenon of impurity-induced layer disordering during the doping of structures with electrically active impurities (donors or acceptors) is well known in the technology of GaAs/AlGaAs quantum structures and has been extensively studied [Deppe and Holonyak (1988); and Laidig *et al.* (1981)]. This phenomenon is connected with the Fermi-level dependence of the formation of excess lattice vacancies or interstitials in the semiconductor crystal lattice which in turn control the disordering [Deppe and Holonyak

---

(1988)]. However, it is believed that the predominant position of  $\text{Er}^{3+}$  ions in the crystal lattice of a III-V semiconductor is the substitutional cation position [Taguchi and Ohno (1995)]. In this case, erbium behaves as an isovalent impurity, i.e. it does not supply (or trap) an additional charge. Therefore we cannot expect that the concentration of erbium ions will influence directly the Fermi level position of the semiconductor, and the explanation of high diffusion coefficients discussed in Deppe and Holonyak (1988) cannot be applied to our results. It should be noted that in our case impurity-induced layer disordering due to the interdiffusion of Ga and Al is observed at a substrate temperature lower by 100-200 K compared to the studies described in Deppe and Holonyak (1988).

The strong diffusion of erbium and interdiffusion of gallium and aluminum may be due to the large difference between the ionic radii of Er and the Ga and Al cations.  $\text{Er}^{3+}$  has a radius of 0.881 Å, while the ions of Ga and Al have radii of 0.62 Å and 0.51 Å respectively [Weast (1974)]. This difference leads to the formation of a significant number of additional cation vacancies and a corresponding increase in the diffusion coefficients of the cations. It is known that the local shear strain induced by the introduction of impurities reduces the energy of the formation of vacancies in the vicinity of an alien atom. This reduction is stronger the greater the difference between the ionic radii of the alien and host ions [Boltaks (1972); and Frenkel (1955)].

The diffusion coefficient is small when erbium is introduced into GaAs by diffusion because the radius of the erbium ion is larger than the gallium radius. The diffusion coefficient of impurities depends also on the concentration of cation or anion vacancies, but since the concentration of vacancies in the equilibrium condition is constant at

constant temperature, it is the size of the impurity atom that determines the diffusion rate. The situation is different in the case when the vacancies are created in the process of growth, and this is what happens in the MBE growth of Er-doped GaAs/AlGaAs structures. As shown in Alves *et al.* (1993) in the case of  $\text{Al}_{0.5}\text{Ga}_{0.5}\text{As}$  prepared by MBE for concentrations up to  $10^{18} \text{ cm}^{-3}$ , 88 percent of erbium ions occupy substitutional positions (the cation site). For higher erbium concentration the fraction of erbium ions in interstitial positions increases, and for  $N_{\text{Er}} = 5 \times 10^{19} \text{ cm}^{-3}$  only 30 percent of erbium is in substitutional positions. (Still we can expect that the deformation induced by an erbium ion in the interstitial position is even larger).

The tendency of erbium to have aluminum nearby is probably due to their chemical interaction since it is known that there exists several intermetallic compounds of erbium and aluminum [Wallace (1973)]. On these grounds we can expect the formation of different erbium-aluminum complexes in our samples.

#### Er- photoluminescence and defects induced by Er

The PL spectrum of the Er21 sample consists of some ten lines. However, having compared the spectra measured at  $T = 5 \text{ K}$  and  $T = 40 \text{ K}$  (Fig. 10) we have observed a sharp difference in the behavior of the intensities of the lines. Some of the lines have dramatically decreased in intensity with increased temperature while others have had almost no change in intensity. We have determined that there are three series of these lines (*a*, *b*, and *c*) according to their temperature quenching.

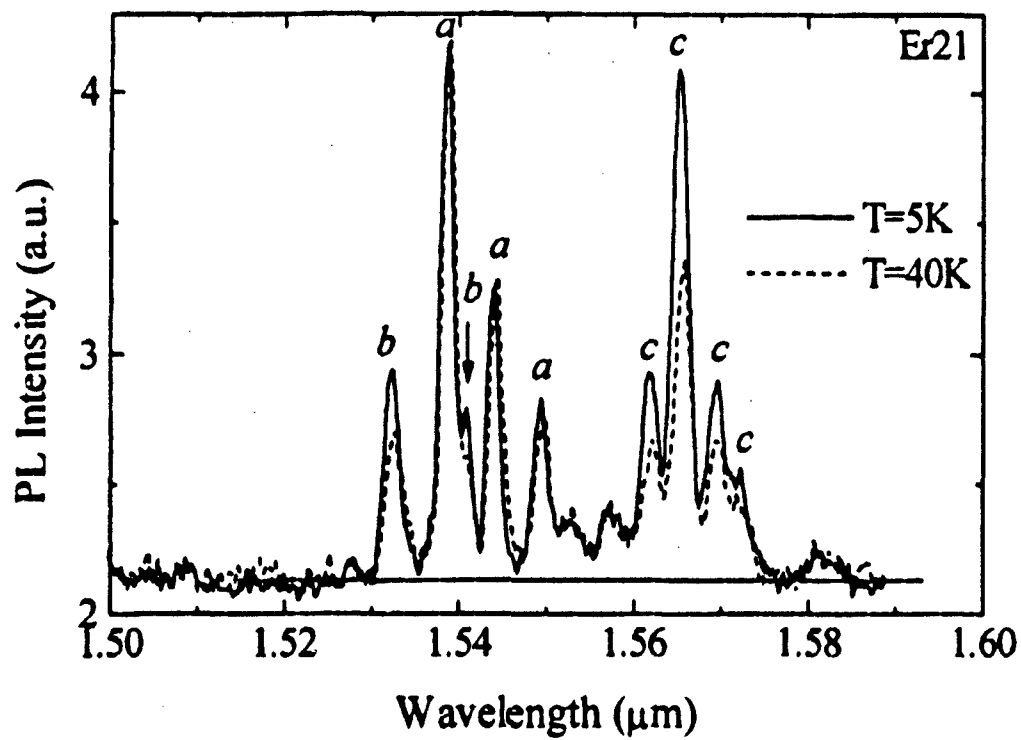


**Figure 10** High resolution PL spectra of Er21 at  $T_1=5\text{K}$  (solid line) and  $T_2=40\text{K}$  (dashed line).

Our measurements of the lifetimes of the erbium ions in the excited state have demonstrated that the lifetime corresponding to the  $a$  line was about 0.5 ms while those for the  $b$  and  $c$  lines were only 0.05-0.07 ms.

In Fig. 11 the PL spectra of two samples with two different concentrations of erbium inserted into their QW's are shown. It is clear that besides the differences in temperature dependence and lifetimes, the  $a$ ,  $b$ , and  $c$  series of lines differ also by their linewidths. The linewidths of the  $b$  and  $c$  series are 15 Å while those in the  $a$  series are less than 7 Å. Also, the ratio of the intensities within each series is constant and independent of the concentration of erbium inserted into the GaAs QW's.

Thus, from the temperature quenching, lifetimes, linewidths of the PL, and the ratios of the lines' intensities in each series we have concluded that the introduction of erbium into AlGaAs leads to the formation of three groups of erbium centers. We propose that the existence of these centers is accompanied by an appearance of three defect levels in the semiconductor bandgap involved in the Auger excitation of the erbium ions. We have labeled these defect levels as  $D_a$ ,  $D_b$ , and  $D_c$ . It follows from the temperature dependence measurements that  $D_a$  is a deep level while  $D_b$  and  $D_c$  are shallow ones.

It is known that the introduction of erbium into a GaAs semiconductor matrix induces the appearance of an impurity potential in the crystal lattice [Elsaesser *et al.* (1995)]. The nature of this isovalent impurity potential is determined both by a difference in the internal (short-range) potentials of the matrix atom and by a difference in their atomic sizes. However, it is generally believed that the differences of the atomic radii



predominates. This fact leads to shear deformation of the lattice resulting in the splitting of the degenerate GaAs valence band. As a result, a potential that attracts holes appears. The origin of the shallow hole trap, with a binding energy of 35 meV in GaAs, which is induced by an introduction of erbium is presumably due to just this reason. If the erbium concentration exceeds  $5 \times 10^{17} \text{ cm}^{-3}$  (the limiting solubility of erbium in GaAs), erbium begins to occupy interstitial positions within the crystal which leads to a formation of a deep defect hole trap with an energy of 350 meV [Elsaesser *et al.* (1993); Elsaesser *et al.* (1995); and Taguchi and Ohno (1995)].

We assume that similar hole traps should also be formed in AlGaAs upon the introduction of erbium, and that their binding energies should be close to those observed in GaAs. In fact, we have found two defect PL lines in the 640–680 nm range at high pump rates, when the intrinsic erbium PL tends towards saturation (Figs. 12 and 13).

In the spectrum of Fig. 12 we can see two fairly wide lines with maxima at  $Db = 1.87 \text{ eV}$  and  $Dc = 1.90 \text{ eV}$  and a narrow exciton line at  $Ex = 1.92 \text{ eV}$ . Using similar reasoning as in the case of GaAs, we can assume that erbium ions in the substitutional positions in AlGaAs induce two shallow defect levels with binding energies of 20 and 50 meV (calculated from the differences in the positions of the exciton line  $Ex$  and the defect PL lines  $Db$  and  $Dc$ ). The existence of two types of shallow traps in AlGaAs instead of only one in GaAs is probably due to the different surroundings of erbium ions in the AlGaAs matrix. It should be noted that we cannot ascribe these defect states unambiguously to hole traps. This point actually requires further study.

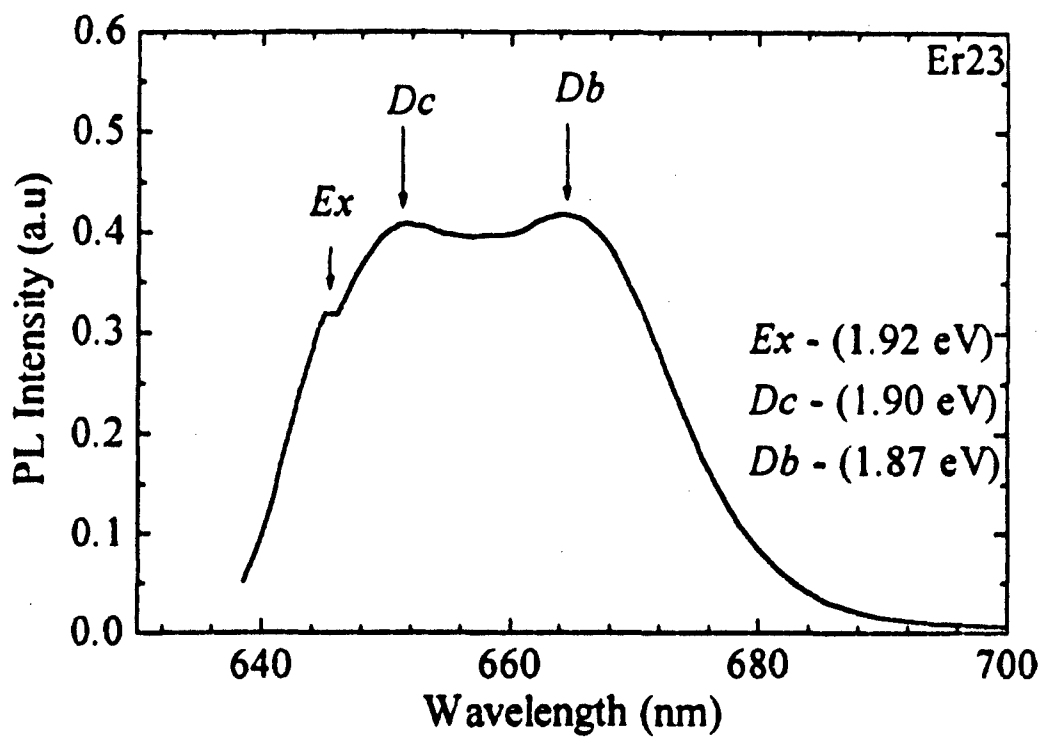


**Figure 12** PL spectrum of Er23 taken at 10.5 K demonstrating the presence of shallow defect states in Er-doped GaAs/AlGaAs.

The results of temperature quenching studies of the *Db* and *Dc* defect lines and *a*, *b*, and *c* erbium series are given in Figs. 13, 14, and 15. The quenching of the defect *Dc* line is significantly stronger than that of the *Db* line (Fig. 13). The activation energy of 65 meV found from the temperature dependence of the *Db* line (Fig. 15a) is in fair agreement with the binding energy of the *Db* level deduced from the PL data:  $1.92 - 1.87 = 0.05$  eV. The temperature quenching of the erbium PL *c* line occurs with an activation energy of 25 meV (Fig. 15a) corresponding to the binding energy of the *Dc* level found from the PL data:  $1.92 - 1.90 = 0.02$  eV.

Thus, the quenching of the erbium PL connected with the most shallow trap *Dc* is controlled by depopulation of this state with rising temperature. As can be seen from Figs. 15a and 15b, the temperature quenching of the *b* and *a* lines of the erbium PL is weaker than that of the *c* line. The effective drop of the line *a* intensity starts only at about 50 K for Er23, and starts at above  $\sim 100$  K for Er29 (AlGaAs). The line *a* can be observed practically up to room temperature. Note, that the temperature quenching of the *b* and *a* lines occurs earlier than we should expect from depopulation of the corresponding defect levels.

It should be noted that the position of the exciton line at  $E_x = 1.92$  eV corresponds to the composition of the alloy  $\text{Al}_x\text{Ga}_{1-x}\text{As}$  with  $x = 0.32$ . However, as we stated earlier, the average composition of  $\text{Al}_x\text{Ga}_{1-x}\text{As}$  that would be obtained as a result of the complete leveling of the gallium and aluminum concentrations over the QW region due to cation interdiffusion could not exceed  $x = 0.25$ . This difference also indicates that there exist erbium-containing clusters enriched by aluminum.

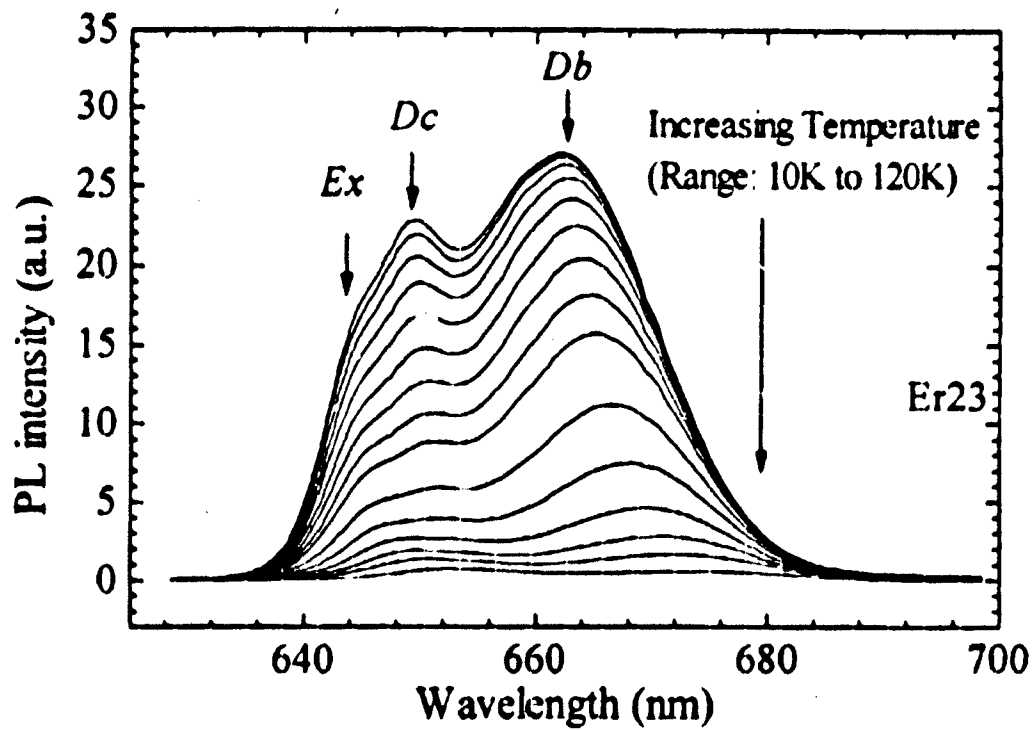


**Figure 13** Temperature evolution of the PL spectra of Er23 demonstrating the temperature quenching of the *Db* and *Dc* defect lines.

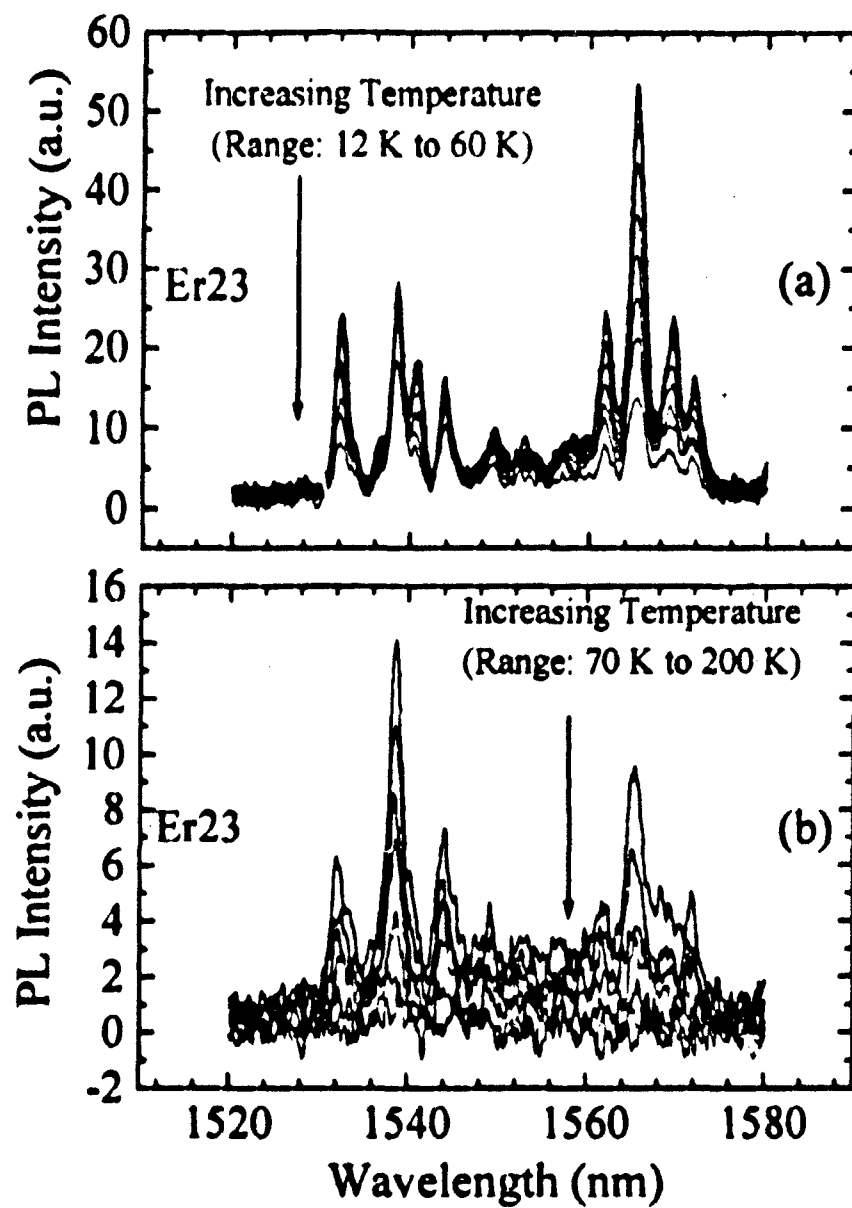


**Figure 14** Temperature evolution of the PL spectra of Er<sub>23</sub> demonstrating the temperature quenching of the *a*, *b*, and *c* lines for the ranges a) 12 K to 60 K and b) 70 K to 200 K.

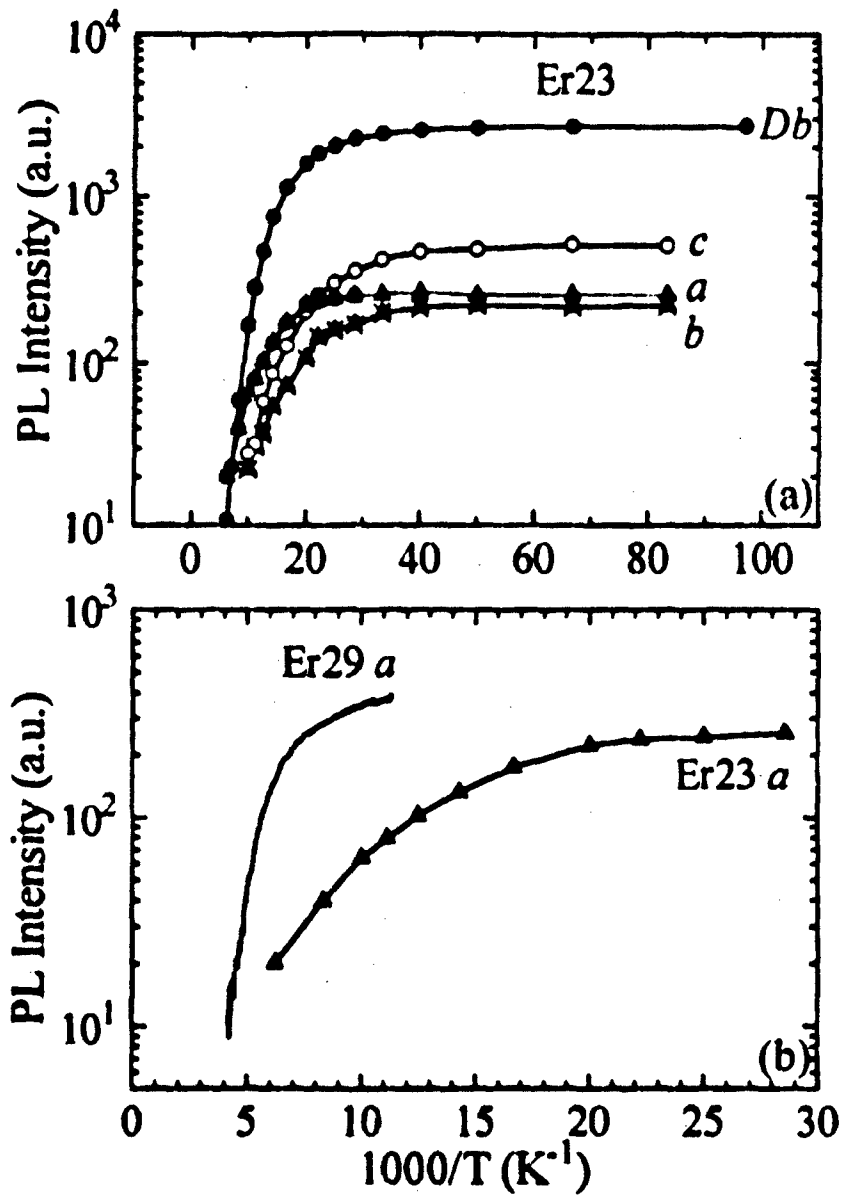


**Figure 15** a) Temperature dependence of the intensities of the *Db* defect line and the erbium *a*, *b*, and *c* lines for Er23.  
 b) Temperature dependence of the intensities of the erbium *a* lines for Er29 and Er23.

In Fig. 16 we show a complete PL spectrum for Er23 in the 800-1800 nm range. Series of narrow lines are distinctly seen at wavelengths of 810, 980, and 1550 nm which correspond to transitions of the  $\text{Er}^{3+}$  ion from three lowest excited states:  ${}^4I_{9/2} \rightarrow {}^4I_{13/2}$  (1.53 eV),  ${}^4I_{11/2} \rightarrow {}^4I_{13/2}$  (1.26 eV), and  ${}^4I_{13/2} \rightarrow {}^4I_{15/2}$  (0.81 eV). Besides the PL band at 640 - 690 nm determined by transitions to the shallow defect traps  $D_b$  and  $D_c$  and the exciton line discussed above, a wide PL band is observed that peaks around 1000 nm. We believe that this band is caused by optical transitions to the deep hole states  $D_a$ . The observation of a wide band probably indicates the existence of a strong electron-phonon interaction for the deep state.

Thus, we have actually found three types of erbium-induced traps in AlGaAs and PL from the upper excited states,  ${}^4I_{9/2}$  and  ${}^4I_{11/2}$ , of the  $\text{Er}^{3+}$  ions.

### ***Discussion of Er-Luminescence Excitation and De-Excitation Mechanism***

#### **Excitation and de-excitation processes of erbium luminescence**

Based on our experimental results, we propose the following model for the excitation of the erbium ion 4f-shell. The pump radiation generates electron-hole pairs in the erbium-containing AlGaAs region. Holes are quickly captured by the hole traps  $D_a$ ,  $D_b$ , and  $D_c$  that were induced by erbium being at the cation sites and interstitials (Fig. 17). Recombination of a free electron and a hole captured by the trap can be: 1) radiative (i.e. the defect PL that was observed by us at high pump rates), 2) nonradiative multiphonon capture of a free electron, or 3) Auger capture of an electron with excitation of the 4f-shell of an erbium ion (Auger excitation). In the latter case the majority of the

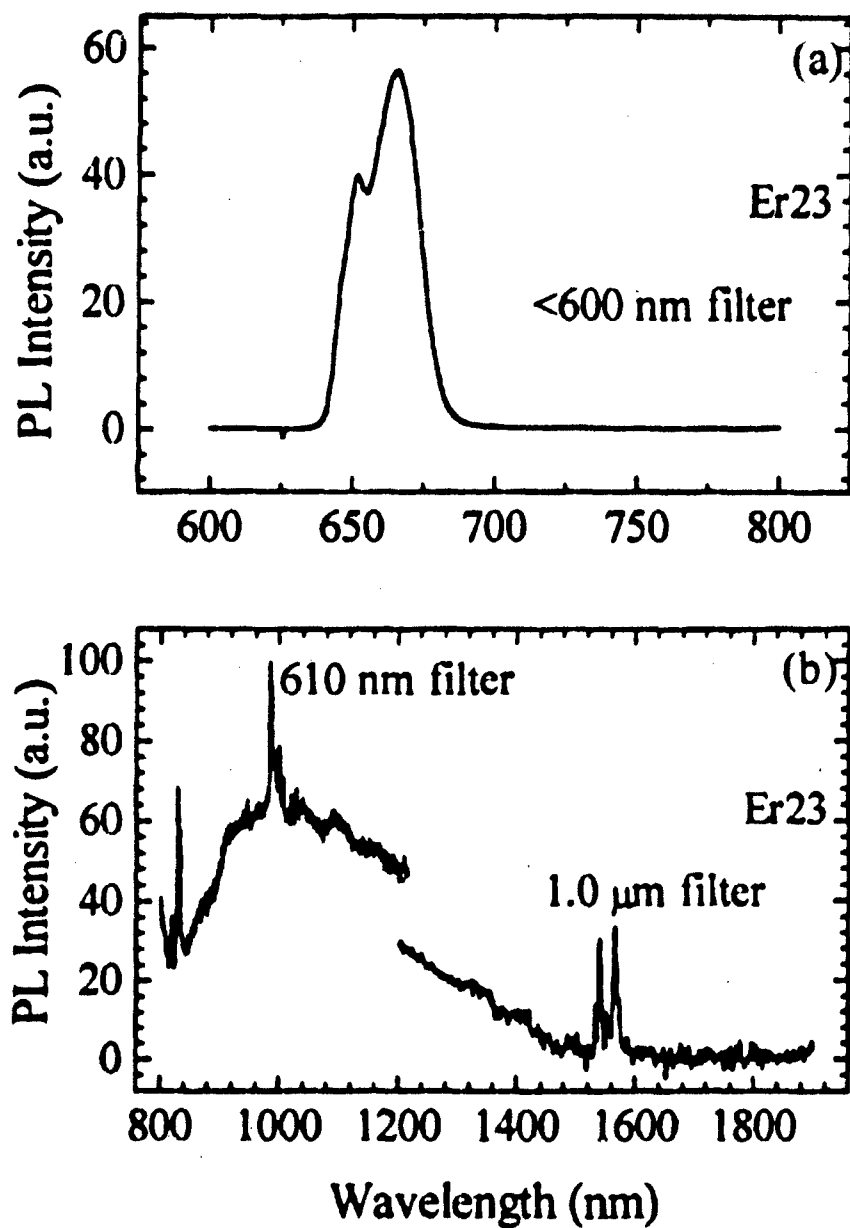


Figure 16 PL spectrum taken at 10 K of Er<sub>23</sub> in a wide spectral range (800-1800 nm).

recombination energy is transferred to the erbium ion to excite the f-shell via a Coulomb interaction.

The probability of the radiative process (process 1) is only slightly temperature dependent. The main contribution to the temperature dependence of the probabilities of processes 2 and 3 is the existence of energy barriers which control the multiphonon processes required to achieve equilibrium. The probability of Auger excitation increases as the energy of the defect PL approaches the excitation energy of the f-f transition (resonance condition).

In the wide-gap AlGaAs alloy the excitation process proceeds via upper states. In this case the reverse process of de-excitation of the erbium ions from the lowest excited state  $^4I_{13/2}$  (the initial state of the 1.54  $\mu\text{m}$  radiative transition) should be negligible. However, de-excitation processes from the upper excited states to which the f-electron is excited in the Auger process can be important. The corresponding probability increases drastically in the resonance condition. The de-excitation process consists of a transition of an f-electron of the erbium ion from the excited to the ground state and a simultaneous generation of an electron-hole pair: a free electron appears in the conduction band while the hole is localized at the defect. If the energy of the electron-hole pair generation exceeds the energy of the f-f transition the energy deficit is compensated by the lattice playing the role of a thermostat.

When the resonance condition is favorable for the excitation process, de-excitation is also enhanced. The fact that the resonance condition is optimal at low temperatures

leads to a sharp temperature quenching of the erbium PL due to de-excitation processes which increase drastically as the temperature rises.

#### Analysis of experimental data

In Fig. 17 a possible diagram for Auger excitation of the erbium ions via deep *Da* and shallow *Db* and *Dc* local states is presented. Since the energies of the defect PL connected with the shallow traps (*Db* and *Dc* lines) are close to the energy of the  ${}^4F_{9/2} \rightarrow {}^4I_{13/2}$  transition, it is reasonable to propose that the excitation occurs via the  ${}^4F_{9/2}$  level. For excitation via the deep trap *Da* we can expect excitation via the  ${}^4I_{11/2}$  and  ${}^4I_{13/2}$  levels. This assumption is confirmed by the observation of erbium PL corresponding to the  ${}^4I_{9/2} \rightarrow {}^4I_{13/2}$  and  ${}^4I_{11/2} \rightarrow {}^4I_{13/2}$  transitions shown in Fig. 16.

The fact that the defect PL (*Da*, *Db*, *Dc*) can be observed only for high excitations, when the erbium PL is saturated, indicates that the probability of Auger excitation is greater than that of the radiative transition.

In the case of the excitation of erbium via shallow traps, the temperature quenching of the erbium PL could be controlled by the thermal depopulation of shallow defect levels. We have actually observed this situation for the line of erbium PL.

In the case of excitation via deep defects *Da* the temperature quenching is no longer determined by the thermal depopulation of the *Da* level. We assume that in this case the temperature quenching of the erbium PL is controlled by competition between the Auger-excitation and multiphonon nonradiative capture. This reason is why we can see a line PL to almost room temperature.

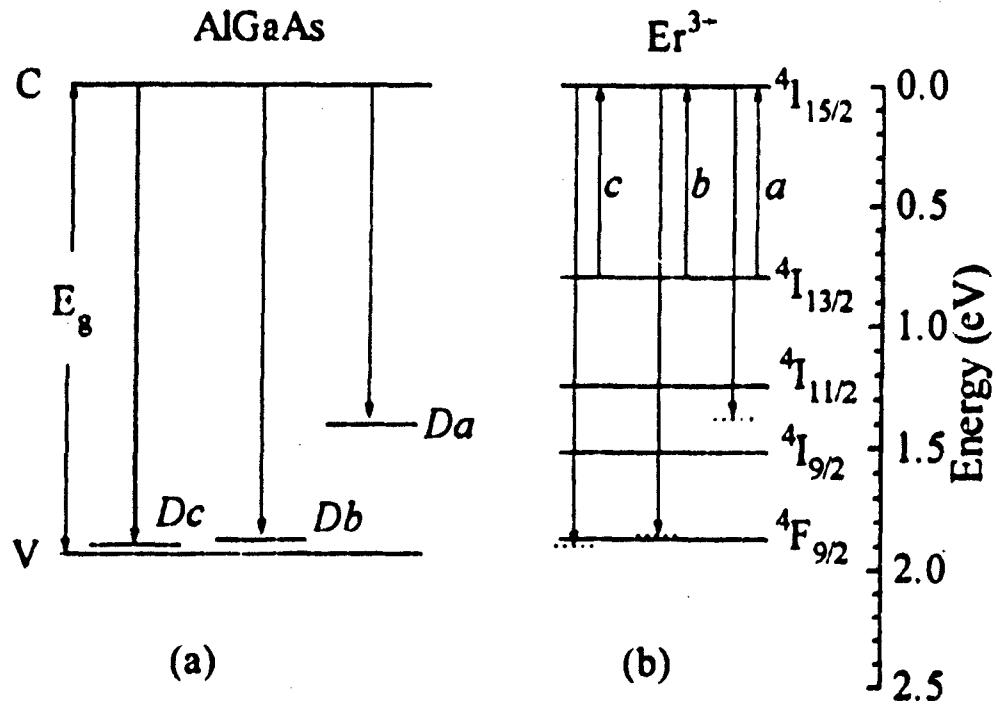


**Figure 17** Energy level diagram and transition scheme for the Auger excitation of erbium ions via  $D_a$ ,  $D_b$ , and  $D_c$  defect centers. For comparison of the defect and f-f transition energies, the positive direction of the energy axis for the  $Er^{3+}$  ion levels is reversed.

### **Conclusions**

In this chapter we have demonstrated that the introduction of erbium into GaAs QW's with AlGaAs barriers during MBE growth leads to strong diffusion of erbium and interdiffusion of gallium and aluminum resulting in leveling of the QW's. These erbium impurities form three types of hole traps in the bandgap of AlGaAs (one of them being deep with a binding energy of about 400 meV, and two shallow ones with energies of 25 and 50 meV). Excitation of the f-shell of the erbium ions in the AlGaAs is determined by an Auger process with the participation of holes captured by the traps, accompanied by excess energy being transferred to local phonons. The temperature quenching of the erbium PL excited via the shallow traps is caused by a thermal depopulation of the defect levels. The temperature quenching of the erbium PL excited via the deep traps is due to an increase in the probability of multiphonon thermally activated capture of free electrons competing with the Auger excitation process. Erbium PL at 1.54  $\mu\text{m}$  excited via a deep trap can be observed nearly up to room temperature. The observation of erbium PL corresponding to the transitions from the  $^4I_{9/2}$  and  $^4I_{11/2}$  levels indicates that a three-level excitation scheme for the PL at 1.54 $\mu\text{m}$  can be realized in erbium-doped AlGaAs.

## Personnel Supported

PI	Galina Khitrova
Co-PI	Hyatt Gibbs
Students	Eric Lindmark, John Prineas
Consultants	Vadim Masterov Irina Yassievich Misha Bresler Oleg Gusev

## Publications

- G. Khitrova, H. M. Gibbs, E. Lindmark, J. Prineas, S. Park, O. B. Gusev, M. S. Bresler, I. N. Yassievich, and V. F. Masterov, "Energy transfer from semiconductor quantum wells to  $\text{Er}^{3+}$ ," APS March Meeting, Bull. APS 41 (1), 139 (1966), St. Louis.
- O. B. Gusev, J. P. Prineas, E. K. Lindmark, M. S. Bresler, G. Khitrova, H. M. Gibbs, I. N. Yassievich, B. P. Zakharchenya, and V. F. Masterov, "Er in MBE-grown GaAs/AlGaAs structures," submitted to J. Appl. Phys.
- E. K. Lindmark, J. P. Prineas, G. Khitrova, H. M. Gibbs, O. B. Gusev, B. Ya. Ber, M. S. Bresler, I. N. Yassievich, B. P. Zakharchenya, and V. F. Masterov, "Er-Induced Ga-Al Interdiffusion in GaAs/AlGaAs Quantum Structures," SPIE Photonics West '97 Proceedings.
- M. S. Bresler, B. Ya. Ber, O. B. Gusev, E. K. Lindmark, J. P. Prineas, H. M. Gibbs, and G. Khitrova, "Er Diffusion and Er-Induced and Er-Induced Ga-Al Interdiffusion in GaAs/AlGaAs Quantum Structures," 19<sup>th</sup> International Conference on Defects in Semiconductors, July 1-25, 1997, Aveiro, Portugal.
- O. B. Gusev, G. Khitrova, E. K. Lindmark, J. P. Prineas, H. M. Gibbs, M. S. Bresler, I. N. Yassievich, and B. P. Zakharchenya, "Er-Induced Defects and Erbium Luminescence in MBE-Grown AlGaAs:Er," 19<sup>th</sup> International Conference on Defects in Semiconductors, July 21-25, 1997, Aveiro, Portugal.
- O. N. Yassievich, M. S. Bresler, O. B. Gusev, and G. Khitrova, "Excitation and De-excitation of Erbium Ions in Semiconductor Matrices," 19<sup>th</sup> International Conference on Defects in Semiconductors, July 21-25, 1997, Aveiro, Portugal.